Molecular Physics
Vol. 109, No. 3, 10 February 2011, 435–446

Taylor & Francis
Taylor & Francis Group

RESEARCH ARTICLE

Long-range damping functions improve the short-range behaviour of 'MLR' potential energy functions

Robert J. Le Roy[a]*, Carl C. Haugen[a], Jason Tao[a] and Hui Li[ab]

[a]*Department of Chemistry, University of Waterloo, Waterloo, ON N2L 3G1, Canada;* [b]*Institute of Theoretical Chemistry, State Key Laboratory of Theoretical and Computational Chemistry, Jilin University, 2519 Jiefang Road, Changchun 130023, PR China*

(*Received 28 July 2010; final version received 21 September 2010*)

The recently introduced [Mol. Phys. **105**, 663 (2007)] 'Morse/long-range' (or MLR) potential energy function is a very flexible form which explicitly incorporates the theoretically predicted inverse-power-sum long-range tail, is smooth and differentiable everywhere, and includes the well depth $\mathfrak{D}_e$, equilibrium distance r_e, and long-range interaction coefficients C_m as explicit parameters. This form is being used increasingly commonly in direct-potential-fit analyses of experimental data. The present work shows that the MLR form can readily accommodate the inclusion of 'damping functions' in the description of the long-range potential tail, and that inclusion of such terms leads to much more realistic short-range extrapolation behaviour. Illustrative applications to the ground electronic states of MgH, Li_2 and ArXe are presented.

Keywords: potential energy function; damping functions; MgH; $Li_2(X)$; ArXe

1. Introduction

It has long been understood that the most comprehensive, compact, and portable way of summarizing what we know about a given molecular state is in terms of an accurate analytic potential function. In recent years the 'potentiology' of developing and testing new and better potential function forms to serve this purpose has earned considerable attention [1–27]. Criteria on which such functions may be judged include: (i) flexibility – ability to provide very accurate potentials, (ii) compactness of form and parameterization, (iii) whether they are explicitly defined in terms of physically interesting parameters such as well depth $\mathfrak{D}_e$ and equilibrium distance r_e, (iv) ability to provide robust and physically realistic extrapolation at long and short distances, (v) incorporation of physically correct inverse-power long-range behaviour, and (vi) global analytic smoothness and differentiability. On these grounds it is arguable that the generalized Morse/Long-Range (MLR) potential function form of [26] is the best and most generally useful potential function form for single minimum potentials which has been introduced to date. However, it too has shortcomings. One of these is the fact that to date (neglecting inter-state coupling [26]), the long-range behaviour of MLR potentials has always been based on a sum of simple inverse-power terms, and has neglected the 'damping' of those terms due to the electron distribution overlap which occurs as atoms approach one another. The second is the fact that at very short range MLR potentials are excessively (and unphysically) steep, with a singularity as $r \to 0$ whose order far exceeds the theoretically predicted r^{-1} 'united-atom limit' behaviour. The present work shows that these two independent shortcomings, one associated with long-range and one with short-range behaviour, are both addressed by the introduction of suitably designed 'damping functions' for inclusion with the inverse-power long-range terms.

2. Improving the Morse/long-range (MLR) potential energy function form

2.1. *The current MLR potential function form*

The current version of the MLR potential energy function form is [26]

$$V_{\rm MLR}(r) = \mathfrak{D}_e\left[1 - \frac{u_{\rm LR}(r)}{u_{\rm LR}(r_e)}\exp[-\beta(r)\cdot y_p^{\rm eq}(r)]\right]^2, \quad (1)$$

*Corresponding author. Email: leroy@uwaterloo.ca

ISSN 0026–8976 print/ISSN 1362–3028 online

DOI: 10.1080/00268976.2010.527304
http://www.informaworld.com

in which $\mathfrak{D}_e$ is the well depth, r_e is the equilibrium internuclear distance, and the radial variable in the exponent is

$$y_p^{eq}(r) \equiv \frac{r^p - {r_e}^p}{r^p + {r_e}^p}. \quad (2)$$

The exponent coefficient $\beta(r)$ is defined so that

$$\lim_{r\to\infty} \beta(r) \equiv \beta_\infty = \ln\{2\mathfrak{D}_e/u_{LR}(r_e)\}, \quad (3)$$

and as a result, the function $u_{LR}(r)$ defines the long-range behaviour of the potential energy function

$$V(r) \simeq \mathfrak{D}_e - u_{LR}(r) + \cdots, \quad (4)$$

while the denominator factor $u_{LR}(r_e)$ is simply the value of that long-range tail function evaluated at the equilibrium bond length. In the most general case, the exponent coefficient function

$$\beta(r) = \beta_p^q(r) \equiv y_p^{ref}(r)\beta_\infty + \left[1 - y_p^{ref}(r)\right] \sum_{i=0}^{N} \beta_i [\, y_q^{ref}(r)]^i \quad (5)$$

is defined in terms of two radial variables which are similar to $y_p^{eq}(r)$, but are defined with respect to a different expansion centre (r_{ref}), and involve two different powers, p and q (the reasons for this structure are discussed in [26]):

$$y_p^{ref}(r) \equiv \frac{r^p - {r_{ref}}^p}{r^p + {r_{ref}}^p} \quad \text{and} \quad y_q^{ref}(r) \equiv \frac{r^q - {r_{ref}}^q}{r^q + {r_{ref}}^q}. \quad (6)$$

In almost all[1] previous work with the MLR potential form, the long-range interaction has been defined as a sum of simple inverse-power terms

$$u_{LR}(r) = \sum_{i=1}^{last} \frac{C_{m_i}}{r^{m_i}}. \quad (7)$$

The limiting long-range behaviour of the exponential term in Equation (1) means that the power p must be greater than $(m_{last} - m_1)$ if the long-range behaviour of Equation (7) is to be maintained [24,26]. There is no analogous formal constraint on the value of q; however, experience dictates that its value should lie in the range $3 \lesssim q \leq p$ [26,27].

2.2. *Shortcomings of the MLR potential function form*

Previous work with predecessors of the current MLR potential form [17–19,22] had grappled with the problem that on extrapolation to large or small distances outside the range of the data used to determine the potential, the values of the exponent coefficient $\beta(r)$ would often drop off sharply and become very large and negative. This would cause the potential to pass through a maximum and turn over [22,28]. Up to that time the relevant potentials had been defined in terms of the single radial variable $y_p^{eq}(r)$ of Equation (2) with $p = 1$, and it was shown that defining it in terms of powers $p > 1$ greatly reduced the propensity for this turnover behaviour [22,28]. It was also found that this turn-over behaviour could be rigorously avoided by using two different polynomial expansion orders in the analogue of Equation (5), N_S for distances $r < r_e$ and N_L for distances $r \geq r_e$, where $N_S < N_L$ [22,29,30]. However, this latter step introduced discontinuities into the high-order derivatives of the potential at the point $r = r_e$ where these two polynomial segments met, and the 'two-segment' aspect of that approach was aesthetically untidy.

A much better solution to the problem of avoiding inner-wall potential function turn-over was provided by the introduction of expansion variables $y_{p/q}^{ref}(r)$ of Equation (6) centred at a distance r_{ref} which is somewhat larger than r_e. This removes (by fixing $N_S = N_L \equiv N$) the high-derivative discontinuities at $r = r_e$, and it also means that significantly fewer exponent expansion coefficients β_i are required to give potential functions of a given accuracy (i.e. N can be much smaller) [26]. However, two problems remain.

If we expand the square in Equation (1), the MLR potential is seen to be a sum of a repulsive and an attractive term:

$$V_{MLR}(r) = \mathfrak{D}_e\left[1 + \left(\frac{u_{LR}(r)}{u_{LR}(r_e)}\right)^2 \exp[-2\,\beta(r)\, y_p^{eq}(r)] - 2\frac{u_{LR}(r)}{u_{LR}(r_e)} \exp\left[-\beta(r)\, y_p^{eq}(r)\right]\right]. \quad (8)$$

Since all three expansion variables $y_p^{eq}(r)$, $y_p^{ref}(r)$ and $y_q^{ref}(r)$ approach the value -1 as $r \to 0$, at small r the exponential factor in the repulsive term in Equation (8) approaches a value of $\exp[2\beta(0)]$ with zero limiting slope. This means that the limiting small-r behaviour of the MLR potential is governed by the factor $\left\{u_{LR}(r)\right\}^2$, which at small r becomes proportional to the square of the highest-order inverse-power term in Equation (7). In other words, at very short distances

$$V_{MLR}(r) \propto 1/r^{2m_{last}}. \quad (9)$$

For a common case in which the long-range potential is represented by the three leading dispersion energy terms with $m = 6$, 8 and 10, this means that the potential energy function would have a singularity of order 20 at $r = 0$. This is physically wrong, since the limiting short-range behaviour of any interatomic

potential energy function is defined by the internuclear repulsion term, $Z_1Z_2\,e^2/(4\pi\epsilon_0 r)$ which has a singularity of order 1. This incipient high-order singularity of an MLR potential presents no problem in the potential well region in which it is most sensitive to the data used to determine its parameters (i.e. its β_i expansion coefficients), since the radial behaviour of the empirically determined exponent coefficient function $\beta(r)$ will ensure that the potential function wall is well-behaved there. However, in the short-range extrapolation region the repulsive wall of such an MLR potential would be unphysically excessively steep. This criticism applies to all MLR potential functions reported to date.

As was mentioned in the introduction, a second shortcoming of the MLR potential form which has been used to date is the fact that its attractive long-range tail has been represented by the simple inverse-power sum of Equation (7).[1] This expression is only valid at distances sufficiently large that overlap of the electronic distributions on the interacting species is truly negligible. For the ubiquitous dispersion energy terms (for which $m = 6, 8, 10, \ldots$), it has long been known that at moderate-to-small distances the strengths of these terms drops off sharply from that inverse-power behaviour [31]. This is a less serious concern for an MLR function than it is for potential function forms which attach a pure inverse-power tail at some fixed distance [20,21], since the exponential term in Equation (1) or (8) can effectively perform such damping. However, it is still not an ideal situation. Fortunately, addressing this second problem in an appropriate manner will also resolve the first.

2.3. *Damping functions*

At internuclear distances which are sufficiently large that overlap of the electron distributions on interacting species can be neglected, perturbation theory shows that long-range intermolecular interactions can be represented by the type of inverse-power sum seen in Equation (7) [32,33]. However, such simple inverse-power sums are known to be asymptotic expansions which diverge for all distances [31,34–36]. On the other hand, the long-range perturbation energy may also be written as a sum of 'non-expanded' interaction energies (T_m) which reduce to the conventional 'expanded' inverse-power form (C_m/r^m) if electron overlap is neglected, and these non-expanded energies do yield convergent sums for all r [31,34,35].[2] For the case of two ground-state H atoms, Figure 1 shows how the actual 'non-expanded' energies diverge from simple inverse-power behaviour (i.e. from linear behaviour on this log/log plot) at small distances. Following the seminal work of Kreek and Meath [31], it has become customary to introduce 'damping functions' $D_m(r) \equiv T_m/(C_m/r^m)$, defined as the ratio of the non-expanded to the expanded interaction energies, and then to represent the corrected long-range (attractive) interaction energy as

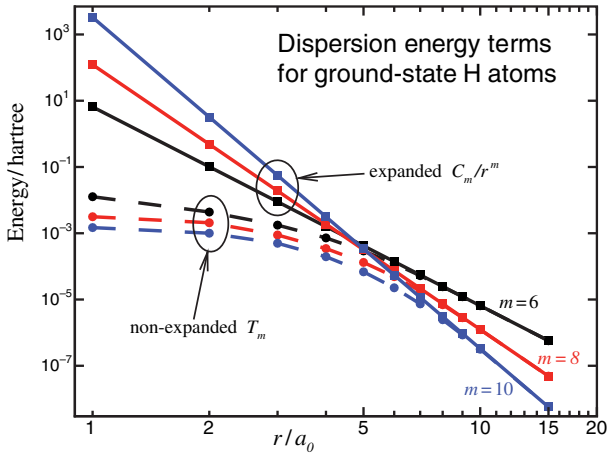

Figure 1. Comparison of 'non-expanded' and 'expanded' dispersion energies for the interaction of two ground-state H atoms, as reported by Kreek and Meath [31].

$$u_{\mathrm{LR}}(r) = \sum_{i=1}^{\mathrm{last}} D_{m_i}(r)\,\frac{C_{m_i}}{r^{m_i}}. \qquad (10)$$

To date, however, damping functions have not been incorporated into the long-range behaviour of most of the model potential function forms used in direct-potential-fit data analysis.

The leading expanded (simple inverse-power terms) and non-expanded dispersion energy terms for two interacting ground-state H atoms reported by Kreek and Meath yield the damping function values shown as points in Figure 2 [31]. Since calculations of non-expanded interaction energies have only been reported for a limited number of few-electron systems, it has become customary to assume that these H_2 results incorporate universal behaviour which may be scaled radially for other molecular systems. As is seen in Figures 1 and 2, at shorter distances electron overlap has the effect of weakening the various terms relative to the simple inverse-power behaviour. This is believed to be generally true for the dispersion energy terms which arise in second-order perturbation theory. We therefore adopt the common approach of assuming that the damping behaviour for all terms contributing to Equation (10) may be mapped onto the behaviour for ground-state H-atoms that was determined by Kreek and Meath [31].

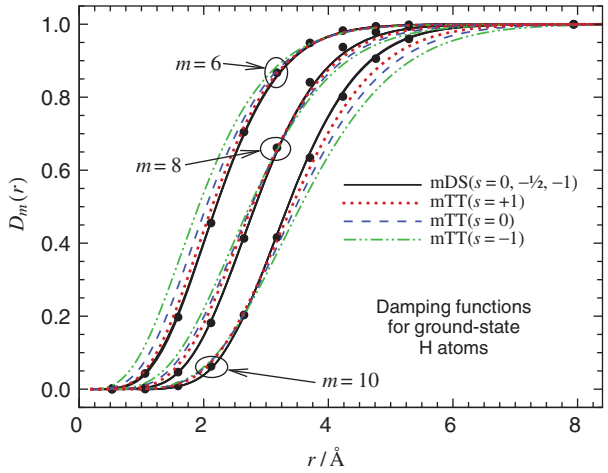

Figure 2. Comparison of modified Tang–Toennies damping functions (mTT) for $s = -1$, 0 and 1 (broken curves) with the modified Douketis *et al.* damping functions (mDS) for $s = 0$, $-\frac{1}{2}$, and -1 (three superimposed solid curves), and with the Kreek–Meath *ab initio* results (solid points).

A damping function form which has been fairly widely used in recent years is one proposed by Tang and Toennies [9]. Unfortunately (see below), it has unphysical short-range behaviour which prevents it from being used within an MLR potential. An alternate function proposed by Douketis *et al.* [37] has better short-range behaviour, but is still not ideal. We therefore generalize these functions to obtain two families of 'modified' damping function forms. Our generalized Douketis *et al.* [37] damping function is

$$D_m^{\mathrm{DS}(s)}(r) = \left(1 - \exp\left(-\frac{b^{\mathrm{ds}}(s)\,(\rho\, r)}{m} - \frac{c^{\mathrm{ds}}(s)\,(\rho r)^2}{m^{1/2}}\right)\right)^{m+s}, \tag{11}$$

and our generalization of the Tang–Toennies [9] damping function is

$$D_m^{\mathrm{TT}(s)}(r) = 1 - \exp[-b^{\mathrm{tt}}(s)\,(\rho r)] \sum_{k=0}^{m-1+s} \frac{[b^{\mathrm{tt}}(s)\,(\rho r)]^k}{k!}. \tag{12}$$

The parameters $b(s)$ and $c(s)$ in Equations (11) and (12) are system-*in*dependent constants determined by optimizing the agreement with the *ab initio* $m = 6$, 8 and 10 damping function behaviour of two ground-state hydrogen atoms (for which case $\rho \equiv 1$, see below) that was determined by Kreek and Meath [31]. The original versions of these functional forms corresponded to the cases $s = 0$ for the Douketis *et al.* [37] form and $s = 1$ for the Tang–Toennies form [9].

Performing least squares fits of these two types of damping functions to the *ab initio* dispersion energy damping factor values for two ground-state H atoms [31] for a range of values of 's' yielded the results presented in Table 1 and Figure 2, where $\overline{dd}$ is the root-mean-square deviations for a given fit. The fact that the generalized Douketis-type functions yield higher quality fits than do the generalized Tang–Toennies forms is to be expected, since they are based on two fitting parameters ($b^{\mathrm{ds}}(s)$ and $c^{\mathrm{ds}}(s)$) rather than one ($b^{\mathrm{tt}}(s)$). Although the quality of fit for the $s = 2$ modified Tang–Toennies forms begins to approach those for the modified Douketis-type functions[3] (that for $s = 3$ is worse), it is not clear that this choice would give the sort of realistic two-parameter van der Waals potentials which have been obtained using the standard $s = 1$ version of these functions [38,39]. In any case, in view of the uncertainties associated with our *ad hoc* extension of these damping function forms to systems other than H–H, this difference in quality of fit is probably not very physically significant. However, it is clear that the $s = 1$ case recommended by Tang and Toennies [9] yields significantly worse agreement with the *ab initio* results than do any of the generalized Douketis-type functions or the generalized Tang–Toennies function for $s = 2$, and within the MLR model, *any* damping function forms for which $s > 0$ are physically unacceptable (see below).

Table 1. Results of fits to Kreek–Meath data [31] using various damping function models. Numbers in parentheses are 95% confidence limit uncertainties in the last digits shown.

	Tang–Toennies		Douketis et al.		
s	$\overline{dd}$	b^{tt}	$\overline{dd}$	b^{ds}	c^{ds}
2	0.0091	3.47(2)	0.0066	4.99(12)	0.34(1)
1	0.018	3.13(3)	0.0064	4.53(12)	0.36(1)
0	0.034	2.78(6)	0.0068	3.95(12)	0.39(1)
$-\frac{1}{2}$	n/a	n/a	0.0073	3.69(13)	0.405(15)
-1	0.055	2.44(8)	0.0078	3.30(14)	0.423(16)
-2	0.081	2.10(10)	0.0094	2.50(16)	0.468(20)

Damping functions were originally devised to take account of the weakening of the simple inverse-power behaviour of dispersion energy terms which occurs when the electron clouds on the the interacting species overlap as the internuclear separation decreases. The size of the electron clouds, and hence the distance at which their overlap becomes 'significant', will of course vary from species to species. This led Douketis *et al.* [37] to introduce a system-dependent range parameter which for interacting atoms A and B has the form

$$\rho \equiv \rho_{AB} = 2\rho_A\rho_B/(\rho_A + \rho_B), \tag{13}$$

in which $\rho_A = (I_p^A/I_p^H)^{2/3}$ is defined in terms of the ratio of the ionization potential of the atom in question (I_p^A) to that of an H atom (I_p^H). This is a physically plausible parameterization which is very convenient to use, since accurate I_p^A values are readily available for all atomic species. Hence, it is adopted here.

2.4. *Short-range behaviour*

The nature of our generalized definitions of the two families of damping functions means that at very small r

$$\lim_{r\to 0}\left\{D_m^{(s)}(r)/r^m\right\} \propto r^s \tag{14}$$

for all values of m and s. The results of Kreek and Meath presented in Figure 1 show that while the damping functions die off at small internuclear distance (see Figure 2), the actual non-expanded interaction energies (damped dispersion energies) monotonically increase in magnitude and approach finite limiting values as $r \to 0$. This implies that the physically most appropriate damping function models are those with $s = 0$. This is the reason that the short-range behaviour of the conventional $s = 1$ Tang–Toennies model was referred to above as being 'unphysical'. If the overall potential function model consists of a simple sum of damped dispersion terms plus a short-range repulsion term, this $s = 1$ limiting behaviour presents no practical problem, since the essential requirement of preventing the attractive inverse-power terms from becoming infinite as $r \to 0$ is still achieved. However when the attractive long-range tail of the potential appears as a multiplicative factor rather than an additive term, as in the case of the MLR potential, other concerns arise.

In the MLR potential function model, the damping functions serve two purposes. The first addresses the usual objective of providing a physically more correct representation of the behaviour of the various long-range terms as the atoms approach one another. The second is associated with the the concern raised in Section 2.2, that if $u_{LR}(r)$ is defined by a sum of simple inverse-power terms, the very short-range behaviour of an MLR potential would be defined by Equation (9). However, Equation (14) shows that if one of our generalized damping functions is used in Equation (10), then at very small distances

$$V_{MLR}(r) \simeq \mathfrak{D}_e\left\{\frac{u_{LR}(r)}{u_{LR}(r_e)}\right\}^2 \exp[2\beta(0)] \propto \left\{u_{LR}(r)\right\}^2 \propto r^{2s}. \tag{15}$$

As was mentioned above, the conventional Tang–Toennies damping function corresponds to the case $s = +1$ [9]. This case, and indeed any damping functions corresponding to any positive value of s, would be completely unacceptable within the MLR form, since Equation (15) indicates that at very small r the repulsive potential wall would turn over and approach zero as $r \to 0$. The present work therefore only considers damping functions corresponding to $s \le 0$. Note that in our generalized Tang–Toennies damping function form s must be an integer, while in the generalized Douketis-type form it may have integer or non-integer values.

The conventional Douketis *et al.* [37] damping function corresponds to Equation (11) with $s = 0$. This is physically acceptable for either an MLR potential or a potential form in which the long-range terms provide a simple additive contribution to the overall interaction. However, setting $s = -\frac{1}{2}$ means that as $r \to 0$, $V_{MLR}(r) \propto 1/r$. As this is the limiting Coulomb repulsion behaviour expected of *all* atom–atom interactions at very short distances, this choice would seem to yield a fortuitous advantage of using this particular damping function form within the MLR model.

It is well known that in the limit of very small interatomic distances, all interatomic potential energy functions take on the 'united atom' (UA) form [40–44]

$$V_{UA}(r) \simeq \frac{Z_A Z_B C_1^{pp}}{r} + E_{AB}^{el}(r) - E_A^{el} - E_B^{el}, \tag{16}$$

in which Z_A and Z_B are the atomic numbers of the interacting atoms A and B, $C_1^{pp} = e^2/4\pi\epsilon_0 = 116140.97\ \text{cm}^{-1}$ Å is the coefficient for the Coulomb repulsion of two protons, E_A^{el} and E_B^{el} are the total electronic energies of isolated atoms A and B, and $E_{AB}^{el}(r)$ is the electronic energy of the united atom with atomic number $Z_A + Z_B$ which is being formed as the two nuclei approach one another. Examination of Equations (1), (5), (10) and (11) for the case $s = -\frac{1}{2}$ shows that at very small r (i.e. as all $y_p(r) \to -1$),

$$V_{MLR}(r) \longrightarrow \frac{\mathfrak{D}_e\left[\exp[\beta(0)]\sum_{i=1}^{\text{last}}\left\{C_{m_i}\left(b^{ds}\rho/m_i\right)^{m_i-\frac{1}{2}}\right\}\Big/u_{LR}(r_e)\right]^2}{r} \equiv \frac{C_1^{sr}}{r}. \tag{17}$$

As a result, an MLR potential defined using modified Douketis *et al.* damping functions for which $s = -\frac{1}{2}$ would automatically take on the limiting very short-range behaviour of Equation (16) if the empirically

determined exponent coefficient function of Equation (5) had the limiting value

$$\beta^{\mathrm{UA}}(r=0) = \ln\left\{\frac{\left[Z_1 Z_2 C_1^{\mathrm{pp}}/\mathfrak{D}_{\mathrm{e}}\right]^{1/2} u_{\mathrm{LR}}(r_{\mathrm{e}})}{\sum_{i=1}^{\mathrm{last}}\left\{C_{m_i}(b^{\mathrm{ds}}\,\rho/m_i)^{m_i-\frac{1}{2}}\right\}}\right\}. \quad (18)$$

However, the limiting behaviour of Equation (16) will only be achieved quantitatively at internuclear distances smaller than the radii of the innermost atomic electrons, and it appears (see below) inconvenient to attempt to impose this constraint in practical applications.

In any case, introduction of any damping function form whose very short-range behaviour is characterized by Equation (14) for a small non-positive value of s both will improve the description of the long-range behaviour, and will prevent the short-range repulsive wall of an MLR potential from taking on the excessively steep unphysical behaviour of Equation (9).

3. Illustrative applications

3.1. *Application to MgH($X\,^2\Sigma^+$)*

A recent study reported a comprehensive analysis of 7453 high-resolution electronic, infrared and microwave data for the ground $X\,^2\Sigma^+$ state of MgH, spanning 99.87% of the potential energy well, which were fully explained by a 'basic' MLR potential energy function with an 18th-order (19-parameter) exponent coefficient function $\beta(r)$ [45]. In the present work this same data set has been reanalysed using, first-of-all, the extended MLR model of [26] with *no* damping functions in $u_{\mathrm{LR}}(r)$, and secondly, using that same extended model with various versions of the generalized damping functions of Equations (11) and (12). The first column of Table 2 presents the parameters of the 'basic' MLR model potential of [24,45],[4] while the second column shows the results obtained from a fit to the same data set which was performed using the extended MLR model of [26] which introduced the shifted expansion centre $r_{\mathrm{ref}} > r_{\mathrm{e}}$ and allows $p \neq q$. The fact that a fit of the same quality is obtained with 4 fewer expansion parameters, and that all of the expansion coefficients have sensible magnitudes of <30 illustrates the advantages of this extended model.

The third column of Table 2 then lists the parameters yielded by a fit to this same MgH data set using an extended MLR model which also included damping functions in the definition of the long-range tail function $u_{\mathrm{LR}}(r)$. As is indicated there, this model achieves essentially the same quality of fit (as measured by the dimensionless root-mean-square deviation $\overline{dd}$) and requires even fewer expansion parameters than did the 'extended'-model potential which did not include long-range damping functions. The results in column 3 were obtained using modified Douketis-type damping functions corresponding to $s=-1$, but results of equivalent quality are obtained using Douketis-type damping functions for $s=0$ or $-\frac{1}{2}$ or using Tang–Toennies-type damping functions corresponding to $s=0$ or -1.

One reason for introducing damping functions into the MLR model was to cause the resulting potential to have more sensible short-range extrapolation behaviour. To examine this question, Figure 3 plots the short-range repulsive walls of potential energy functions for MgH obtained either using no damping functions, or using one of five models mentioned above. For all of these cases the potential functions are essentially identical in the potential well region spanned by the data used to define these potentials (i.e. at negative energies, not shown). However, they clearly have very different short-range extrapolation behaviour. In particular, as predicted by Equation (9), when no damping functions are included in the definition of $u_{\mathrm{LR}}(r)$ the short-range repulsive wall is extremely steep, with (for this case) a limiting short-range r^{-20} behaviour. In contrast, use of damping function models corresponding to various values of s leads to the limiting short-range behaviour predicted by Equation (15).

To provide an objective test of the short-range extrapolation behaviour yielded by these different models, *ab initio* calculations at the multiconfiguration self-consistent field (MCSCF) level [46,47] and high quality multi-reference averaged quadratic coupled-cluster (MR-AQCC) calculations [48] that include dynamic electron correlation effects and size-extensive modifications, were used to generate the interaction energy values shown, respectively, as solid-round and open-square points on Figure 3. Large core-valence basis sets cc-pCV5Z [49] with all electrons correlated were employed, and all of these *ab initio* calculations were performed using the MOLPRO package [50]. In addition, the limiting very-short-range united-atom-limit behaviour implied by Equation (16) is shown in Figure 3 as a dotted line with a slope (on this log/log plot) of -1. The ideal potential function extrapolation behaviour would be to have an $s=-\frac{1}{2}$ potential curve tangentially approaching this dotted line from below as $r\to 0$. However, the only model with the correct limiting short-range functional behaviour (modified-Douketis-type damping with $s=-\frac{1}{2}$) has an effective C_1^{sr} coefficient which is an order of magnitude smaller than the limiting theoretical value of $12C_1^{\mathrm{pp}}$. On the other hand, the short-range repulsive wall obtained when using the modified Douketis-type damping

Table 2. Parameters defining three MLR potential models determined for the $X\,^2\Sigma^+$ state of MgH, and one determined for the $X\,^1\Sigma_g^+$ state of Li_2. The quantity $\overline{dd}$ is the dimensionless root-mean-square deviation for the data analysis fit. Numbers in parentheses are 95% confidence limit uncertainties in the last digits shown.

	MgH($X\,^2\Sigma^+$)}			$Li_2(X\,^1\Sigma_g^+)$
Model	'Basic' MLR[a,b]	No damping[b]	With damping[b,c]	With damping[d]
$\mathfrak{D}_e$/cm^{-1}	11104.70 (5)	11104.71 (3)	11104.26 (8)	8516.708 (4)
r_e/Å	1.729684 (2)	1.729685 (2)	1.7296850 (1)	2.672992 (2)
C_6/cm^{-1} Å^6	2.793×10^5	2.7755×10^5	2.7755×10^5	[6.71527×10^6]
C_8/cm^{-1} Å^8	3.475×10^6	3.4549×10^6	3.4549×10^6	[1.12588×10^8]
C_{10}/cm^{-1} Å^{10}	–	4.614×10^7	4.614×10^7	[2.78604×10^9]
Damping	None	None	DS($s=-1$)	DS($s=-1$)
ρ	n/a	n/a	0.810	0.540
$\{p, q\}$	{4, 4}	{5, 4}	{5, 4}	{5, 3}
r_{ref}/Å	r_e	2.27	2.73	4.07
β_0	−2.33868946	−2.49358518	1.15466294	0.13905144
β_1	−0.77492121	0.0478255	1.040803	−1.431068
β_2	−1.205737	0.6072206	2.6614613	−1.501106
β_3	−0.588667	2.285738	2.548605	−0.65906
β_4	−0.82808	3.294444	0.82066	0.32995
β_5	−0.70793	4.34585	0.27288	1.02588
β_6	−0.8799	3.86759	0.8841	1.2058
β_7	3.5388077×10^3	2.3773	−2.2375	1.1927
β_8	-6.4267393×10^4	−2.8646	−8.2069	3.014
β_9	5.5105233×10^5	−5.518	−6.666	6.568
β_{10}	-2.88176326×10^6	7.850	2.836	0.844
β_{11}	1.01119112×10^7	22.836	6.74	−11.28
β_{12}	-2.4862471×10^7	1.23	2.72	2.41
β_{13}	4.356976×10^7	−27.8		26.4
β_{14}	-5.431477×10^7	−17.6		6.3
β_{15}	4.7147×10^7			−23.5
β_{16}	-2.712×10^7			−14.0
β_{17}	9.3×10^6			
β_{18}	-1.44×10^6			
$\overline{dd}$	0.755	0.756	0.757	1.0044

Notes: [a]The MLR potential function model of [45] for which the exponent polynomial order was $N = N_S = 6$ for $r < r_e$ and $N = N_L = 18$ for $r \geq r_e$.[4]
[b]The centrifugal Born–Oppenheimer breakdown (BOB) radial strength function had two more terms than were used in [45].[4]
[c]To complete the description of this (recommended) model, the dimensionless centrifugal BOB correction parameters are (with p_{na}=3): $t_0^H - t_8^H = 0.0$, 0.0009636, 0.0002, 0.00199, 0.0033, −0.0131, 0.0046, 0.117, and −0.121, while Λ-doubling radial strength parameters were fixed at the values given in [45].
[d]The BOB parameters for the $X\,^1\Sigma_g^+$ state and all of the parameters for the $A\,^1\Sigma_u^+$ state were held fixed at the values reported in [26].

functions with $s = -1$ is clearly in quite good agreement with the *ab initio* results over most of the range considered in Figure 3.

3.2. *Application to* $Li_2(X\,^1\Sigma_g^+)$

A recent study reported a comprehensive analysis of 17,477 data for the $X\,^1\Sigma_g^+$ and $A\,^1\Sigma_u^+$ states of Li_2 which were fitted to 'extended' (i.e. with $r_{ref} > r_e$ and $q < p$) MLR potential energy functions with a 16th-order exponent coefficient function for each state [26]. That analysis has now been repeated while including damping functions in the definition of $u_{LR}(r)$ for the $X\,^1\Sigma_g^+$ state. This yielded the revised parameter set shown in the last column of Table 2 and the short-range extrapolation results shown in Figure 4. In this case, the exponent polynomial order is the same as that for the published undamped model, but the quality of fit is very slightly better ($\overline{dd} = 1.0044$ versus 1.0059). For this system, the $u_{LR}(r)$ model for the $A\,^1\Sigma_u^+$ state is defined in terms of a 2×2 diagonalization [26], and both the A-state potential and the Born–Oppenheimer breakdown (BOB) function models for both states were left unchanged. The value of the damping range-scaling parameter for this species is $\rho = 0.540$.

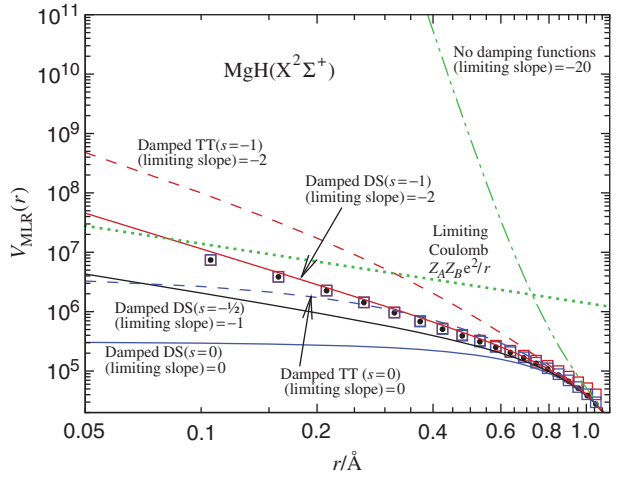

Figure 3. Comparison of short-range extrapolation behaviour of MLR potentials for ground-state MgH which incorporate different types of damping behaviour. All potentials (in units cm^{-1}) came from fits of equal quality to discrete spectroscopic data which span essentially the whole potential well region: $1.3 \lesssim r \lesssim 5.6$ Å. The points were generated from *ab initio* calculations (see text).

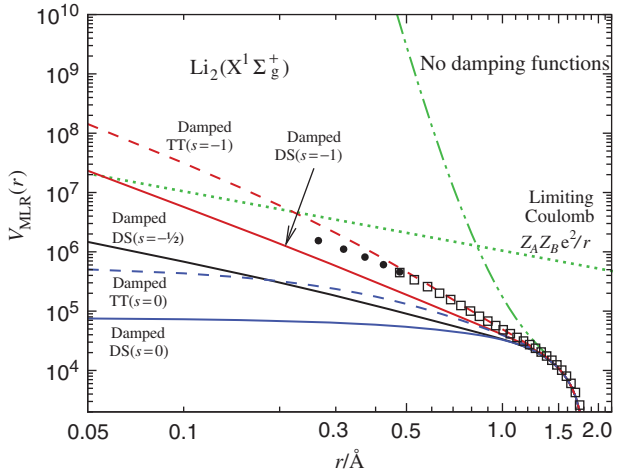

Figure 4. Comparison of short-range extrapolation behaviour of MLR potentials for ground-state Li_2 which incorporate different types of damping behaviour. All potentials (in units cm^{-1}) came from fits of equal quality to discrete spectroscopic data which span essentially the whole potential well region: $1.82 \lesssim r \lesssim 12.52$ Å. The points were generated from *ab initio* calculations (see text).

Figure 4 compares the short-range extrapolation behaviour of the published MLR potential for this state (green dash-dot-dot curve) with those for potentials obtained from equivalent-quality fits to the same data set which used potentials incorporating the five indicated types of damping-functions in the definition of $u_{LR}(r)$ (solid and dashed curves). As in Figure 3, the dotted line shows the limiting short-range behaviour predicted by Equation (16), while the open and solid point were obtained from *ab initio* calculations performed at the MCSCF level with cc-pV5Z and cc-pVQZ [51] basis sets for two lithium atoms.[5] As in Figure 3, those *ab initio* results approach the dotted line from below as $r \to 0$. As for MgH, the limiting short-range behaviour of the potential incorporating $s = -\frac{1}{2}$ modified-Douketis-type damping corresponds to an effective limiting C_1^{sr} coefficient which is an order of magnitude smaller than the limiting theoretical value of (for this case) 9 C_1^{pp}. For this system, it appears that use of the $s = -1$ modified-Tang–Toennies damping function gives a potential which most closely agrees with the *ab initio* results in the short-range extrapolation region.

3.3. *Application to ArXe($X\ ^1\Sigma^+$)*

A very recent study of the the $X\ ^1\Sigma^+$ state of ArXe reported the determination of an MLR potential function incorporating the $s = -1$ version of the modified Douketis-type damping function of Equation (11) [52]. The data set used therein consisted of microwave data for the $v = 0$ levels of five zero-nuclear-spin isotopologues, high resolution VUV emission into vibrational levels $v = 0$ and 1 of $Ar^{132}Xe$ and $Ar^{136}Xe$, and interaction virial coefficients for temperatures ranging from 173 to 695 K. While the turning points of the spectroscopically observed levels only span the range $3.8 \lesssim r \lesssim 4.6$ Å, the virial coefficients are sensitive both to the whole potential well and to the potential wall up to energies of at least 500 cm^{-1}. Since the nature of the bonding in this system is completely different than that for the ground states of MgH and Li_2, it seems useful to present comparative results for this case too.

The recommended potential energy function for this system determined in [52] was an MLR function with two fitted β_i coefficients whose long-range tail $u_{LR}(r)$ was defined by three inverse-power terms (with $m = 6$, 8 and 10) and the $s = -1$ modified Douketis-type damping functions of Equation (11) with $\rho = 1.007$. The short-range repulsive wall of this recommended potential is shown as the solid red curve in Figure 5, while the repulsive walls of five analogously-determined potentials incorporating other types of long-range damping behaviour (solid and dashed curves) or no damping functions (dash-dot-dot curve) are shown there too. As with the other systems considered above, these six potential functions are essentially indistinguishable in the well

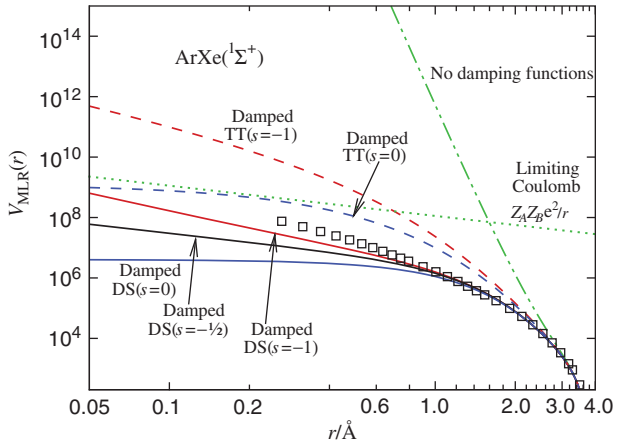

Figure 5. Comparison of short-range extrapolation behaviour of MLR potentials for ground-state ArXe which incorporate different types of damping behaviour. All potentials (in units cm^{-1}) came from fits of equal quality to discrete spectroscopic data which span the region $3.8 \lesssim r \lesssim 4.6$ Å and interaction virial coefficients for $T = 173$–695 K which are sensitive both to the whole potential well and to the short-range repulsive wall up to energies $\sim 500\,cm^{-1}$. The points were generated from *ab initio* calculations (see text).

(negative energy) region. However, to obtain an equivalent representation of the experimental data using a potential function with *no* damping functions included in $u_{LR}(r)$ required one more exponent expansion coefficient (β_2) than did the models which included damping.

The *ab initio* calculations for this system were performed using single- and double-excitation coupled-cluster theory with a noniterative perturbation treatment of triple excitations [CCSD(T)] [53,54]. The basis set used for Ar was aug-cc-pVQZ [55] and that for Xe was the contracted aug-cc-pVQZ basis set, and relativistic 28-core-electron ECP28MDF pseudopotentials were employed for Xe [56].

The pattern of the various curves shown in Figure 5 is qualitatively the same as those for MgH and Li_2. While the function utilizing modified Douketis-type damping for $s = -\frac{1}{2}$ again approaches the theoretically predicted limiting slope of -1, the effective coefficient C_1^{sr} is again more than an order of magnitude smaller than that associated with the limiting behaviour predicted by Equation (15). As for MgH, use of the $s = -1$ Douketis-type damping functions yielded the best agreement with the *ab initio* results.

4. Discussion and conclusions

All previous work with MLR model potential energy functions has been based on long-range tail functions $u_{LR}(r)$ which ignored damping, and were comprised of pure inverse-power terms.[1] However, the present work shows that the MLR form can readily accommodate any damping function form for which the limiting short-range power in Equation (14) corresponds to $s \leq 0$. The present work also provides improved models for the potential energy functions for ground electronic states of MgH and Li_2.

It would be nice if there were an unambiguous choice for the optimum type of damping function, but the results of Figures 3–5 suggest that the situation is not entirely clear. However, in view the excellent agreement with the benchmark H_2 results shown in Table 1 and Figure 2, and the reasonably good agreement with the *ab initio* results seen in Figures 3–5, we are inclined to recommend the $s = -1$ modified Douketis-type function of Equation (11) for preferential use within the MLR potential function form. At the same time the results in Figures 3–5 show that even at supra-thermal collision energies of up to 10^4 cm^{-1}, the extrapolated repulsive potential-function walls yielded by all five of the damping function models considered here are essentially equivalent.

In contrast with the above, when no damping is incorporated into the long-range tail function in the MLR form, the resulting fitted MLR potentials (dash-dot-dot curves in Figures 3–5) have unphysically steep repulsive walls which cross above the predicted limiting behaviour (the dotted lines in Figures 3–5) at relatively large distances. This also affects the compactness of the resulting representation of the potential energy function. In particular, Table 2 shows (cf. columns 3 and 4) that inclusion of damping allowed us to obtain a good description of the MgH data which required two fewer fitting parameters than did an otherwise-equivalent fit using a model with no damping functions. Similarly, when damping functions are omitted from the model potential used in the ArXe data analysis, three rather than two exponent coefficients are required to give a fully satisfactory fit. For the case of Li_2, the exponent polynomial order required to give a fully satisfactory fit remained the same when damping functions are used, but the quality of the resulting fit improved slightly relative to that for the published undamped potential ($\overline{dd} = 1.004$ here versus 1.006 in [26]).

The reason that a higher-order exponent polynomial tends to be required when damping functions are not included in the definition of the MLR long-range tail function $u_{LR}(r)$ is shown by the upper panel of Figure 6. We see there that when no damping functions are used (dashed curves), the exponent coefficient function $\beta(r)$ must drop off sharply at small distances to counter the incipient high-order singular behaviour

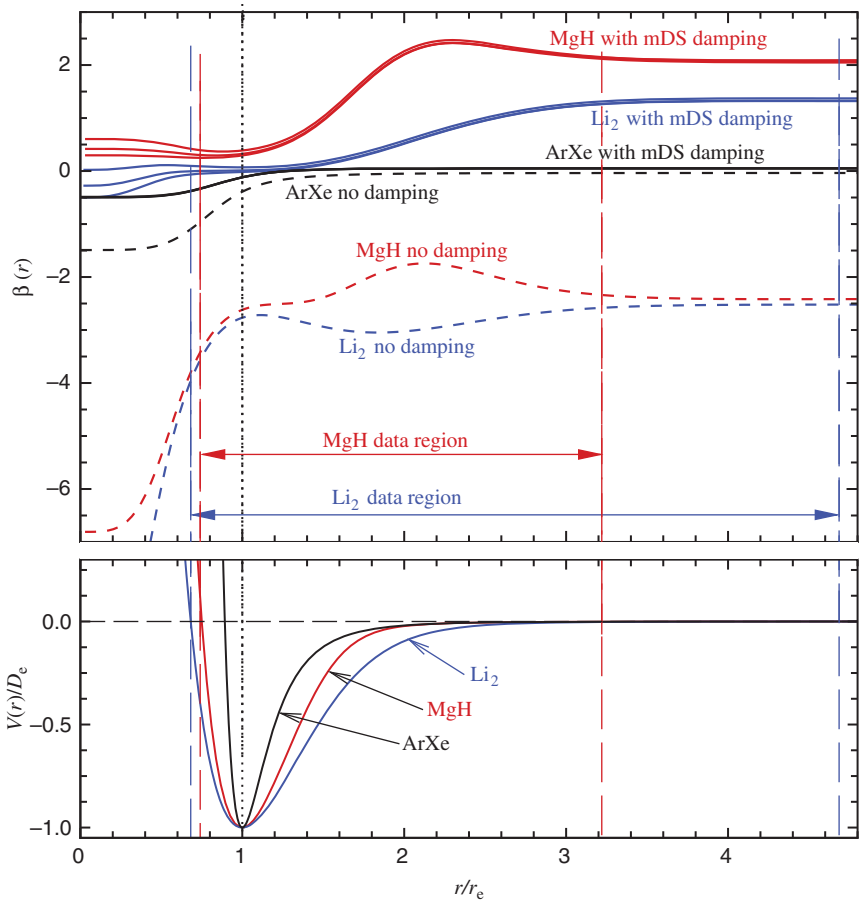

Figure 6. Lower panel: reduced potential energy functions for ground-state MgH, Li_2 and ArXe, plotted versus relative distance r/r_e. Upper panel: exponent coefficient functions $\beta(r)$ determined from direct potential fits using MLR model potentials with (solid curves) and without (dashed curves) inclusion of damping functions in $u_{LR}(r)$. For MgH and Li_2 the three solid curves at short range correspond to (from top to bottom) $s = 0$, $-\frac{1}{2}$, and -1, while for ArXe the curves for these three cases are indistinguishable across the whole range.

of Equation (9). The fact that no such abrupt steep drop-off is required when damping functions are used (solid curves in the upper panel of Figure 6) indicates why fewer $\beta(r)$ expansion coefficients will often be required when long-range damping is incorporated into the MLR potential function form.

From a purely theoretical point of view, an ideal family of damping functions would be one for which $s = -\frac{1}{2}$ and the limiting value of the exponent coefficient function as $r \to 0$ was very near the value of $\beta^{UA}(r = 0)$ defined by Equation (18), as this would mean that $V(r)$ incorporated the limiting united-atom-limit behaviour of Equation (16). However, for all of the cases considered here the empirically determined limiting coefficient C_1^{sr} was an order of magnitude smaller than the theoretically predicted limiting value of $Z_A Z_B C_1^{pp}$. It is is tempting to think of imposing a second limiting constraint on the exponent coefficient function $\beta(r)$ to require it to achieve the limiting value $\beta^{UA}(r = 0)$ as $r \to 0$. However, in terms of the exponent coefficient plots of Figure 6, this would require all of the solid $\beta(r)$ curves in the upper panel of Figure 6 to rise abruptly by 1–2 units in the narrow interval between the inner end of the data-sensitive region and $r = 0$. This could not be achieved readily without substantially increasing the order of the exponent-coefficient polynomial of Equation (5). Thus, we decided to forgo attempting to incorporate the theoretically predicted limiting behaviour of Equation (16) into the MLR potential function form. This is not a serious loss in any practical sense, since Born–Oppenheimer breakdown would require the electrons and nuclei to be treated on an equal basis at interaction energies far below those where Equation (16) could be expected to become valid.

In conclusion, we see that inclusion of damping functions in the form of the long-range tail term $u_{LR}(r)$ in the MLR potential function form has three effects:

- it provides a more physically correct description of the long-range potential tail,
- it provides a more physically realistic description of the extrapolated short-range repulsive potential function wall, and
- the resulting potential function model will often be more compact, requiring fewer parameters to achieve a given quality of agreement with experimental data than would otherwise be necessary.

The only other families of potential function forms which have been shown to have sufficient flexibility to be equally capable of representing extensive, high-resolution spectroscopic data sets are the 'spline-pointwise' potential (SPP) form developed by Pashov and co-workers [20,57,58] and the polynomial-type potentials developed by the Hannover group [21,59,60]. However, use of those forms always requires a substantially larger number of fitting parameters [24,61], and those forms lack the global analytic smoothness and differentiability of the present MLR functions; moreover, their short- and long-range extrapolation behaviour has to be imposed in an *ad hoc* manner.

The most significant remaining shortcoming of the MLR potential energy function form is the fact that it has not been shown to be capable of treating species with double-minimum or 'shelf' potentials accurately, while the SPP form developed by Pashov and co-workers can readily treat such cases [20,57,58]. However, work in progress suggests that this shortcoming may be remedied by merging features of the MLR and SPP potential forms [62].

Acknowledgements

We are pleased to acknowledge helpful discussions with Professors F.R.W. McCourt and M. Nooijen. This research was supported by the Natural Sciences and Engineering Research Council of Canada (NSERC).

Notes

1. The one exception is the treatment of the $A\,^1\Sigma_u^+$ state of Li_2 in [26], for which $u_{LR}(r)$ is determined by diagonalizing a matrix of simple inverse-power terms associated with two coupled states.
2. The terminology 'expanded' versus 'non-expanded' reflects the fact that the derivation of Equation (7) is based on the assumption that the Coulomb interaction between the electrons of one atom and the electrons and nucleus of the other could be expanded in terms of inverse powers of the internuclear separation.
3. On the scale of Figure 2, most of the curves corresponding to modified Tang–Toennies damping functions for $s=2$ are indistinguishable from the curves for the three sets of modified Douketis-type functions. However, the modified Tang–Toennies functions for $s=3$ give a distinctly worse fit for which $\overline{dd}=0.014$.
4. The parameter values shown here differ slightly from those reported in [45] because it was later found that additional terms should have been included in the expression describing the centrifugal Born–Oppenheimer breakdown radial strength function, and that extended model is used here.
5. It is necessary to use different basis sets for the two atoms in order to avoid linear correlation of the basis sets at very short range.

References

[1] Y.H. Pan and W.J. Meath, Mol. Phys. **20**, 873 (1971).
[2] G. Simons, R.G. Parr and J.M. Finlan, J. Chem. Phys. **59**, 3229 (1973).
[3] K.D. Jordan, J.L. Kinsey and R. Silby, J. Chem. Phys. **61**, 911 (1974).
[4] K.D. Jordan, Int. J. Quant. Chem. Symp. **9**, 325 (1975).
[5] A.J. Thakkar, J. Chem. Phys. **62**, 1693 (1975).
[6] J.N. Huffaker, J. Chem. Phys. **64**, 3175 (1976).
[7] R. Engelke, J. Chem. Phys. **70**, 3745 (1979).
[8] J.F. Ogilvie, Proc. Roy. Soc. (London) A **378**, 287 (1981).
[9] K.T. Tang and J.P. Toennies, J. Chem. Phys. **80**, 3726 (1984).
[10] K.T. Tang and J.P. Toennies, Z. Phys. D – At. Mol. Clusters **1**, 91 (1986).
[11] A.A. Šurkus, R.J. Rakauskas and A.B. Bolotin, Chem. Phys. Lett. **126**, 356 (1986).
[12] E. Tiemann, Mol. Phys. **65**, 359 (1988).
[13] W. Hua, Phys. Rev. A **42**, 2524 (1990).
[14] M. Gruebele, Mol. Phys. **69**, 475 (1990).
[15] J.A. Coxon and P.G. Hajigeorgiou, J. Mol. Spectrosc. **139**, 84 (1990).
[16] H.G. Hedderich, M. Dulick and P.F. Bernath, J. Chem. Phys. **99**, 8363 (1993).
[17] P.G. Hajigeorgiou and R.J. Le Roy, *49th Ohio State University International Symposium on Molecular Spectroscopy* (The Ohio Dtate University, Columbus, Ohio, 1994), Paper WE04.
[18] P.G. Hajigeorgiou and R.J. Le Roy, J. Chem. Phys. **112**, 3949 (2000).
[19] E.G. Lee, J.Y. Seto, T. Hirao, P.F. Bernath and R.J. Le Roy, J. Mol. Spectrosc. **194**, 197 (1999).
[20] A. Pashov, W. Jastrzębski and P. Kowalczyk, Comp. Phys. Comm. **128**, 622 (2000).
[21] C. Samuelis, E. Tiesinga, T. Laue, M. Elbs, H. Knöckel and E. Tiemann, Phys. Rev. A **63**, 012710 (2000).
[22] Y. Huang and R.J. Le Roy, J. Chem. Phys. **119**, 7398 (2003), erratum: *ibid* **126** 169904 (2007).

[23] L. Chen and J. Yang, J. Chem. Phys. **127**, 124104 (2007).
[24] R.J. Le Roy and R.D.E Henderson, Mol. Phys. **105**, 663 (2007).
[25] O. Zehnder and F. Merkt, J. Chem. Phys. **128**, 014306 (2008).
[26] R.J. Le Roy, N. Dattani, J.A. Coxon, A.J. Ross, P. Crozet and C. Linton, J. Chem. Phys. **131**, 204309 (2009).
[27] J.A. Coxon and P.G. Hajigeorgiou, J. Chem. Phys. **132**, 094105 (2010).
[28] R.J. Le Roy and Y. Huang, J. Mol. Struct. (Theochem) **591**, 175 (2002).
[29] R.J. Le Roy, D.R.T Appadoo, K. Anderson, A. Shayesteh, I.E. Gordon and P.F. Bernath, J. Chem. Phys. **123**, 204304 (2005).
[30] R.J. Le Roy, D.R.T Appadoo, R. Colin and P.F. Bernath, J. Mol. Spectrosc. **236**, 178 (2006).
[31] H. Kreek and W.J. Meath, J. Chem. Phys. **50**, 2289 (1969).
[32] H. Margenau, Rev. Mod. Phys. **11**, 1 (1939).
[33] J.O. Hirschfelder, C.F. Curtiss and R.B. Bird, *Molecular Theory of Gases and Liquids* (Wiley, New York, 1964).
[34] F.C. Brooks, Phys. Rev. **86**, 92 (1952).
[35] A. Dargarno and R. McCarroll, Proc. Roy. Soc. (London) **A 237**, 383 (1956), *ibid* **A 239**, 413 (1957).
[36] A. Koide, J. Phys. B **9**, 3173 (1976).
[37] C. Douketis, G. Scoles, S. Marchetti, M. Zen and A.J. Thakkar, J. Chem. Phys. **76**, 3057 (1982).
[38] K.T. Tang and J.P. Toennies, J. Chem. Phys. **118**, 4976 (2003).
[39] D.D. Yang and K.T. Tang, J. Chem. Phys. **131**, 154301 (2009).
[40] R.A. Buckingham, Trans. Faraday Soc. **54**, 453 (1958).
[41] W.A. Bingel, J. Chem. Phys. **30**, 1250 (1959).
[42] W. Byers Brown, Disc. Faraday Soc. **40**, 140 (1965).
[43] W. Byers Brown and E. Steiner, J. Chem. Phys. **44**, 3934 (1966).
[44] R.K. Pathak and A.J. Thakkar, J. Chem. Phys. **87**, 2186 (1987).
[45] A. Shayesteh, R.D.E Henderson, R.J. Le Roy and P.F. Bernath, J. Phys. Chem. A **111**, 12495 (2007).
[46] H.-J. Werner and P.J. Knowles, J. Chem. Phys. **82**, 5053 (1985).
[47] P.J. Knowles and H.-J. Werner, Chem. Phys. Lett. **115**, 259 (1985).
[48] P.G. Szalay and R.J. Bartlett, Chem. Phys. Lett. **214**, 481 (1993).
[49] D.E. Woon, K.A. Peterson, T.H. Dunning Jr, private communication (2005).
[50] MOLPRO is a package of *ab initio* programs written by H.J. Werner, P.J. Knowles, R.D. Amos, A. Berning, D.L. Cooper, M.J.O. Deegan, A.J. Dobbyn, F. Eckert, S.T. Elbert, C. Hampel, R. Lindh, A.W. Lloyd, W. Meyer, A. Nicklass, K. Peterson, R. Pitzer, A.J. Stone, P.R. Taylor, M.E. Mura, P. Pulay, M. Schutz, H. Stoll, and T. Thoorsteinsso.
[51] J.T.H Dunning, J. Chem. Phys. **90**, 1007 (1989).
[52] L. Piticco, F. Merkt, A.A. Cholewinski, F.R. McCourt, R.J. Le Roy, J. Mol. Spectrosc. (2010, in press).
[53] C. Hampel, K.A. Peterson and H-J. Werner, Chem. Phys. Lett. **190**, 1 (1992).
[54] M.J.O. Deegan and P.J. Knowles, Chem. Phys. Lett. **227**, 321 (1994).
[55] D.E. Woon and T.H. Dunning, J. Chem. Phys. **98**, 1358 (1993).
[56] K. Peterson, D. Figgen, E. Goll, H. Stoll and M. Dolg, J. Chem. Phys. **119**, 11113 (2003).
[57] A. Pashov, W. Jastrzębski and P. Kowalczyk, J. Chem. Phys. **113**, 6624 (2000).
[58] A. Pashov, W. Jastrzębski, W. Jaśniecki, V. Bednarska and P. Kowalczyk, J. Mol. Spectrosc. **203**, 264 (2000).
[59] O. Allard, C. Samuelis, A. Pashov, H. Knöckel and E. Tiemann, Eur. Phys. J. D **26**, 155 (2003).
[60] E.J. Salumbides, K.S.E Eikema, W. Ubachs, U. Hollenstein, H. Knöckel and E. Tiemann, Eur. Phys. J. D **47**, 171 (2008).
[61] R.J. Le Roy, in *Equilibrium Structures of Molecules*, edited by J. Demaison and A.G. Csaszar (Taylor & Francis, London, 2010), Ch. 6, pp. 168–211.
[62] See, J. Tao, R.J. Le Roy and A. Pashov, presented at the *65th International Symposium on Molecular Spectroscopy*, Columbus, Ohio, June 21–25, 2010, Paper MG07.